REVIEW ARTICLE

Recent Progress of Photosensitive Polyimides

Photosensitive polyimides (PSPIs) have been attracting great attention as insulating materials in microelectronic industry, and can be directly patterned to simplify processing steps. This review highlights recent developments on PSPIs, divided into two major categories; positive-working and negative-working. Especially, lithographic chemistries of PSPIs are focused up to pattern formation as well as other functionalities such as low-temperature imidization.

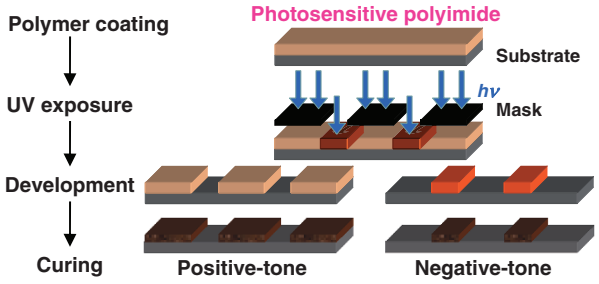

K. FUKUKAWA and M. UEDA
Vol. 40, No. 4, pp 281–296 (2008)

SHORT COMMUNICATION

Use of Fluorescence-Labelled Macroinitiator to Investigate Nucleation Mechanism in Nitroxide-Mediated Crosslinking Polymerization in Aqueous Miniemulsion

The particle formation mechanism in nitroxide-mediated crosslinking copolymerization of styrene and divinylbenzene in aqueous miniemulsion has been investigated by use of a novel technique based on fluorescence-labelling of a polystyrene-TEMPO macroinitiator. The molecular weight distributions of the polymer obtained were analyzed by gel-permeation chromatography using fluorescence- and refractive index detection. The results show that for the TEMPO-mediated miniemulsion copolymerization of styrene and divinylbenzene under the present conditions, particle formation occurs exclusively *via* monomer-droplet nucleation, and secondary nucleation can be neglected.

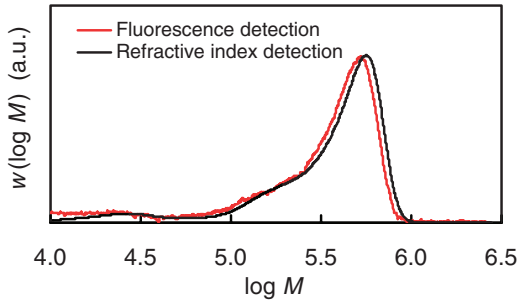

P. B. ZETTERLUND, Md. N. ALAM, and M. OKUBO
Vol. 40, No. 4, pp 298–299 (2008)

Inducing Rapid Crystallization of Slowly-crystallizable Copolyester by *in situ* Generation of Crystalline Nuclei in Melt of Copolyester

Polarized light microscopy images of samples (A) P(3HB), (B) P(3HB)/BN(2 wt %), (C) P(3HB-*co*-21 mol %3HH), (D) P(3HB-*co*-21 mol %3HH)/BN(2 wt %), (E) P(3HB-*co*-21 mol %3HH)/P(3HB)(10 wt %) and (F) P(3HB-*co*-21 mol %3HH)/P(3HB)(10 wt %)/BN(2 wt %). BN is an effective nucleating agent for P(3HB) but not for P(3HB-*co*-21 mol %3HH). It was found that in P(3HB-*co*-21 mol %3HH)/P(3HB)/BN ternary blend, the BN particles at first induce the accelerated crystallization of P(3HB), and then *in situ* produced P(3HB) crystalline particles induce the rapid crystallization of P(3HB-*co*-21 mol %3HH).

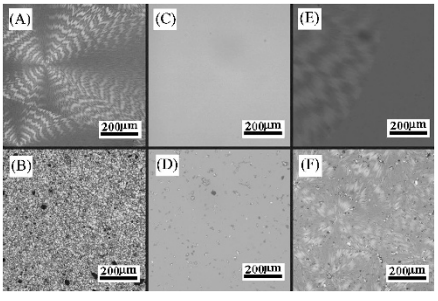

K. TAJIMA, T. DONG, K. HIROSE, T. AOYAMA, and Y. INOUE
Vol. 40, No. 4, pp 300–301 (2008)

Polymer Journal

REGULAR ARTICLE

Trivalent Metal Adsorption Properties on Synthesized Viscose Rayon Succinate

Viscose rayon succinate (VRS) was synthesized from viscose rayon and succinic acid and in the presence of dimethylsulfoxide. The peaks corresponded to carboxyl groups at 1734 cm^{-1}, carboxyl groups with metal ions in the range of 1605–1639 cm^{-1} were certified FT-IR spectra after esterification, adsorption of metals, respectively. The adsorption of the metal ions on the VRS increased when the pH increased. An equilibrium model was modified using basic chemical potentials and the Boltzmann distribution for predicting the adsorption.

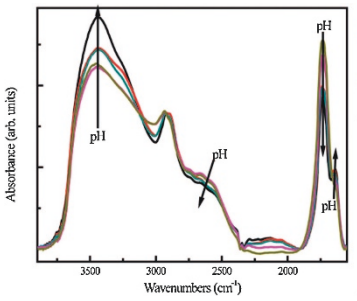

$$\frac{n_{(RCOO)_3Cr}}{3P(A)n_{RCOO^- max} - 9P(A)n_{(RCOO)_3Cr} + n_{(RCOO)_3Cr}} = \frac{K_{effect}}{27} C_{Cr^{3+}} 10^{3pH} \exp\left(\frac{2F\Psi_0}{RT}\right)$$

	Cr^{3+}	Al^{3+}	Fe^{3+}
Max. ads. (mmol/g)	1.48	1.059	1.029
P(A)	0.10959	0.1099	0.10909
χ	0.38715	0.10354	0.33695
K_{effect}	0.03617	0.30952	0.78282
$\Psi_o (mV)$	-1.6296	-1.6296	-1.6296

A. D. KHASBAATAR, Y. J. CHUN, and U. S. CHOI
Vol. 40, No. 4, pp 302–309 (2008)

A Novel Thermal Curing Reaction of Oxetane Resin with Active Diester

Thermal curing reactions of oxetane resins [mixtures of novolac type oxetane (PNOX) with 2,2′-bis[(3-ethyl-3-oxetanyl)methoxy]biphenyl (2,2′-BPOX) and of [4-[(3-ethyl-3-oxetanyl)-methoxy]phenyl]methane (THPMOX) with 2,2′-BPOX] with active ester, 4,4′-isopropylidenebis(2,6-dichlorophenyl diacetate) (IBDCPA) were examined using tetraphenylphosphonium chloride (TPPC) as a catalyst in bulk, and it was found that the reactions proceeded smoothly at 170–190 °C to produce insoluble gel products in good yields.

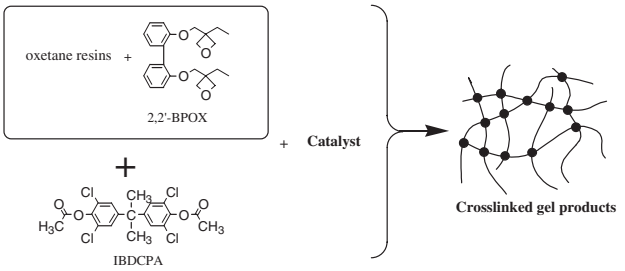

T. NISHIKUBO, H. KUDO, and H. NOMURA
Vol. 40, No. 4, pp 310–316 (2008)

Polysilane Organogel with Hierarchical Structures Formed by Weak Intra-/Inter-chain Si/FC and van der Waals Interactions

Semiflexible polysilane copolymer bearing 3,3,3-trifluoropropyl and *n*-decyl side chains formed organogels in nonpolar organic solvents by weak intra/interchain Si/FC and van der Waals interactions.

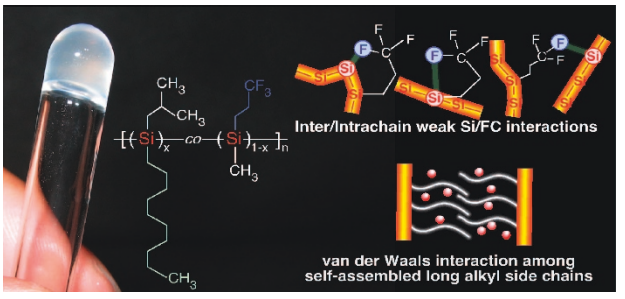

T. KAWABE, M. NAITO, and M. FUJIKI
Vol. 40, No. 4, pp 317–326 (2008)

Utilization of DNA-metal Ion Biomatrix as a Relative Humidity Sensor

Recently, we prepared the novel biomatrix by the mixing of DNA and metal ion. So, we proposed the humidity sensor for the novel utilization of DNA-metal ion biomatrix. The biomatrix with the humidity property was prepared by the mixing of DNA and metal ion. These matrices indicated the different color with the change of relative humidity (RH). These biomatrices may have a potential for the novel RH sensor with flexibility, low cost, non-hazardous, biodegradable, and environmentally benign.

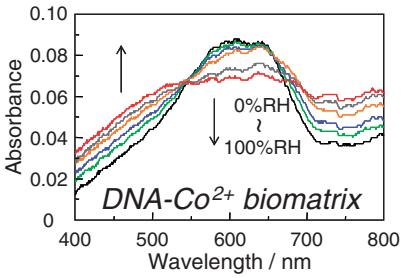

M. YAMADA and T. SUGIYAMA
Vol. 40, No. 4, pp 327–331 (2008)

Precipitation Polymerization of 2-Methylene-1,3-dioxepane in Supercritical Carbon Dioxide

Free radical homopolymerization of 2-methylene-1,3-dioxepane and copolymerization 2-methylene-1,3-dioxepane and *N*-vinyl-2-pyrrolidone were conducted with in supercritical carbon dioxide ($scCO_2$) using a heterogeneous precipitation polymerization method and AIBN as the initiator. We also estimated monomer reactivity ratio and investigated the effect of reaction temperature on the reactivity ratios of 2-methylene-1,3-dioxepane and *N*-vinyl-2-pyrrolidone. Finally submicron sized fine particles of copolymer were obtained from ASES process.

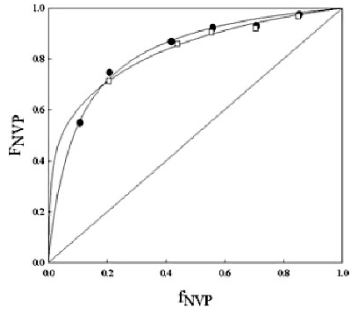

S. KWON, K. LEE, W. BAE, and H. KIM
Vol. 40, No. 4, pp 332–338 (2008)

Growth and Disappearance of Nanobubbles during the Foaming of Polycarbonate

Numerous CO_2 nanobubbles having a size of around 50 nm were obtained at an early stage of polycarbonate foaming. However, most of the initially formed nanobubbles disappeared during the foaming before growing to large ones on a micrometer scale because of coalescence and Ostwald ripening.

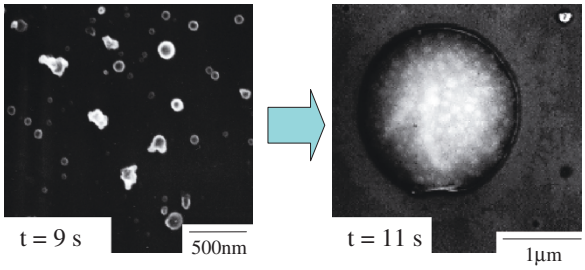

Y. FUKASAWA, H. SAITO, M. KATO, T. CHIBA, and T. INOUE
Vol. 40, No. 4, pp 339–342 (2008)

Polymer Journal

Conformational Analysis of Ethylene Oxide and Ethylene Imine Oligomers by Quantum Chemical Calculation

Conformational analyses have been carried out for ethylene oxide (EO) and ethylene imine (EI) oligomer (x = 1–11 mer) by quantum chemical calculations (RHF/6-31+G(d,p)). $(tg^+t)_x$ structures agreed with those observed by XRD for PEO or PEI crystals. However, some parameters in both helices did not agree with observed values. Each difference was estimated by effect of intermolecular interactions in polymers. For $(tg^+t)_x$ of EI-11, the existence of metastable skewed helices (reversed: a, and kinked: c) were estimated in addition to helix: b.

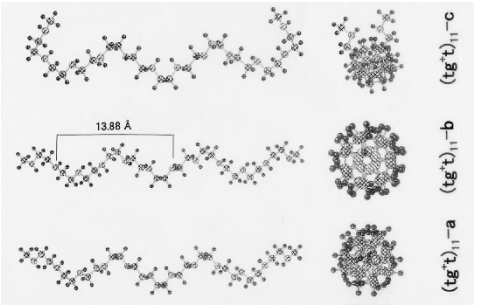

M. KOBAYASHI and H. SATO
Vol. 40, No. 4, pp 343–349 (2008)

The Effects of Small Contents of Water on Melt Rheology for Ethylene-Methacrylic Zinc Ionomers

The effects of small contents of absorbed water on coordinated structure and rheological properties for EMAA-Zn ionomers in term of dynamic visocoelastic and FT-IR measurement were investigated. Figure shows that zero shear viscosities of EMAA-ionomers were reduced by small contents of absorbed water when neutrization degree is larger than 40%. This effect was led by coordination structure change around zinc ions by small amount of water.

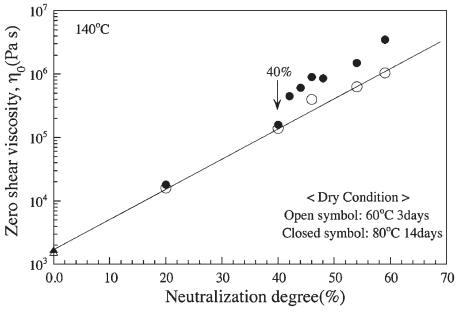

A. NISHIOKA, T. KODA, K. MIYATA, G. MURASAWA, and K. KOYAMA
Vol. 40, No. 4, pp 350–353 (2008)

Soluble Polyimides Based on Long-chain Alkyl Groups *via* Amide Linkages

The synthesis and characterization of a novel series of soluble polyimides, based on *N*-alkyl-3,5-diaminobenzamide (ADBA-9∼14), and the polyimides based on *N*-(3,5-diaminophenyl)-3,4,5-tris(alkoxy)benzamide (DPABA-6,12) are described. Polyimides based on BTDA and ADBA-9∼14 were insoluble, however, copolyimides based on BTDA, ADBA-9∼14, and DDE were soluble. The polyimides and copolyimides based on BTDA, DPABA-6 or DPABA-12, and DDE, containing 50 mol % or more DPABA were soluble. Above polyimides and copolyimides were soluble in various polar solvents and exhibited good heat-resistance.

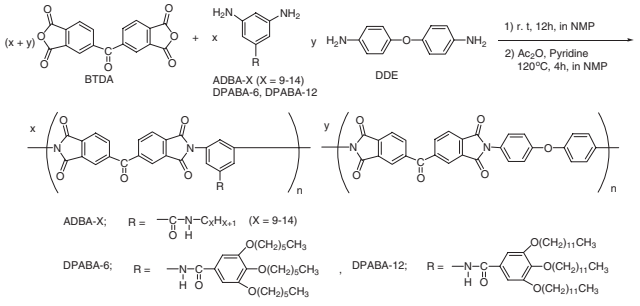

Y. TSUDA, M. KOJIMA, T. MATSUDA, and J. M. OH
Vol. 40, No. 4, pp 354–366 (2008)

Polymer Journal

Laser-Induced Reversible Volume Phase Transition of a Poly(*N*-isopropylacrylamide) Gel Explored by Raman Microspectroscopy

We demonstrate that photon pressure can trigger volume phase transition of a gel. A micro-rod of poly(*N*-isopropylacrylamide) (PNIPAM) in a D_2O solvent undergoes reversible shrinkage/swelling induced by a focused near infrared (1064 nm) laser beam. The local structure of the rod of gel upon laser-induced shrinkage was investigated in detail by means of spatially-resolved micro-Raman spectroscopy. The dynamics of the phase transition was also investigated. Light would be an alternative tool to control a gel.

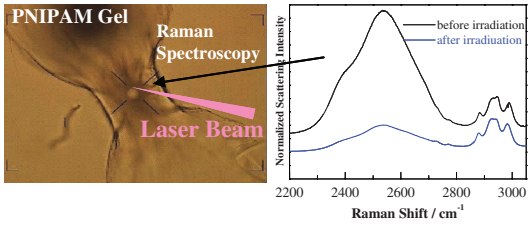

Y. TSUBOI, M. NISHINO, and N. KITAMURA
Vol. 40, No. 4, pp 367–374 (2008)

NOTE

On the Dimension of a Hyperbranched Polymer Synthesized from a Styrene Derivative

The hydrodynamic radius of polystyrene-like hyperbranched polymer was larger than that of liner polystyrene with the same degree of polymerization, because of the differnce of local strucutre of polymer chains.

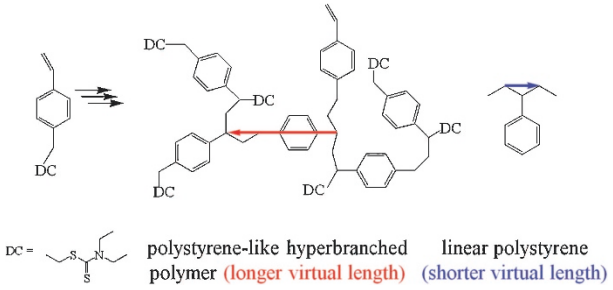

Y. MATSUDA, M. KOBAYASHI, A. TAKAHARA, A. TANAKA, H. HAYASHI, M. ANNAKA, and T. SATO
Vol. 40, No. 4, pp 375–378 (2008)

Fabrication of Large Nanomembranes by Radical Polymerization of Multifunctional Acrylate Monomers

Large, free-standing nanomembranes (thickness, 20–30 nm) were fabricated by radical photopolymerization of acrylate component alone. Densely cross-linked structure and/or rigid backbone produce sufficient mechanical strength to retain the free-standing feature. These acrylate nanomembranes are free-standing in air with the size of 3 cm^2. Reflection of light by the nanomembrane is clearly seen on the left side.

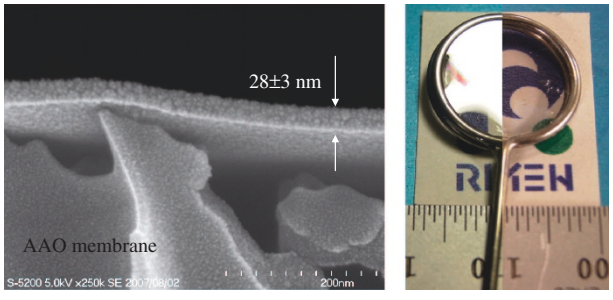

H. WATANABE, T. OHZONO, and T. KUNITAKE
Vol. 40, No. 4, pp 379–382 (2008)